Journal of Engineering and Applied Science Vol. 08, No. 02, pp. 107–114, December 2024

Journal of Engineering and Applied Science

Contents are available at www.jeas.ruet.ac.bd

Investigation of volatile corrosion inhibitors using a facile method

Md. Badiuzzaman Biddut, Nushrat Jahan Rinky, Md Mayeedul Islam*

Department of Chemistry, Rajshahi University of Engineering & Technology, Bangladesh

ARTICLE INFORMATION

Received date: 17th Oct 2024
Revised date: 29th Dec 2024
Accepted date: 29th Dec 2024

Keywords

Volatile corrosion inhibitors (VCIs), Vapor phase corrosion (VPC), Top-of-the-line corrosion (TLC), Vapour inhibiting ability (VIA), Weight loss.

ABSTRACT

Top-of-the-line corrosion (TLC), a significant form of vapor phase corrosion (VPC), is a major concern in oil and gas transportation pipelines operating under stratified flow conditions. Conventional inhibitors used in these pipelines cannot reach the top portion due to their low volatility. In this study, a novel experimental setup was developed to investigate TLC. Azole-based compounds were initially screened and subsequently evaluated for their effectiveness in inhibiting TLC using this new setup. The experiments were conducted at 30 °C surface temperature and at varying gas temperatures of 40 °C, 50°C and 60°C. The results demonstrate that the setup is capable of accurately measuring TLC, water condensation rates, and droplet retention time, while also providing precise control over sample surface and gas temperatures. A Vapor Inhibiting Ability (VIA) test identified benzothiazole as a more effective VPC inhibitor compared to 2-aminothiazole and 2-mercaptobenzothiazole. Benzothiazole was found to reduce TLC by 80% under CO_2 conditions. Additionally, a new spectroscopic method was proposed to measure the concentration of VCIs in the condensed liquid, revealing that a significant amount of VCI co-condensed with the liquid.

1. Introduction

Corrosion is the degradation of materials, typically metals, resulting from chemical or electrochemical reactions with their environment. When alloys are exposed to a corrosive environment and come into contact with oxygen (O_2) and water (H_2O), they corrode on the anodic side through oxidation. Corrosion affects various industries, including ships, pipelines, turbines, and aircraft, having a significant impact on the global economy [1].

Carbon steel is a widely used alloy due to its broad mechanical strength, high machinability, and availability. However, this useful material is susceptible to vapor phase corrosion (VPC) when exposed to oxygen, moisture, or atmospheric pollutants such as carbon dioxide (CO_2), hydrogen sulfide (H_2S), dust, soot, and radiation [2]. In particular, during the transportation of unprocessed wet gas from offshore platforms to onshore processing plants, water vapor in the gas phase can condense on the internal pipeline surface. This occurs due to the temperature gradient and heat exchange between the warm gas and the external environment. The condensed water, saturated with CO_2, H_2S, and volatile organic acids, leads to corrosion in the upper portion of the steel pipeline (typically between the 10 o'clock and 2 o'clock positions), a phenomenon known as top-of-the-line corrosion (TLC) [3,4].

* Corresponding authors: Department of Chemistry, Rajshahi University of Engineering & Technology, Bangladesh
E-mail addresses: mayeedul@chem.ruet.ac.bd (Md. Mayeedul Islam)

TLC is particularly concerning because the stratified flow regime in wet gas pipelines hinders the transport of corrosion inhibitors to the top of the pipeline. In this flow pattern, the liquid phase remains at the bottom, while the gas phase occupies the top. Conventional corrosion inhibitors are ineffective against TLC because their low vapor pressure prevents them from reaching the upper portion of the pipeline.

Mitigating VPC remains a challenge, as no perfect solution has been developed yet. Various methods have been attempted over the decades, such as using corrosion-resistant alloys like stainless steel for pipeline construction. However, this option is significantly more expensive than traditional materials. Another approach involves applying thick insulation coatings to reduce the temperature gradient between the inner and outer walls of the pipeline, thereby decreasing water condensation and TLC rates. However, these coatings require frequent maintenance, and there is a risk of corrosion under the insulation. Additionally, batch applications of inhibitors using "pigs"—devices that spray inhibitors inside the top portion of pipelines—are common. However, this method is not suitable for all pipelines, and pigs can get stuck or require production shutdowns for maintenance [5].

Recent studies suggest that volatile corrosion inhibitors (VCIs) could be a promising solution for mitigating VPC due to their relatively high vapor pressure, which allows them to reach the top of the line, co-condense with water, and form a protective film on the metal surface [6,7]. Azole derivative compounds are heterocyclic molecules containing π electrons, polar groups, and heteroatoms like nitrogen, oxygen, and sulphur. They can create co-ordination bond with metal surface by donating lone pair electron [8,9,10]. While conventional long-chain hydrocarbons can prevent bottom-line corrosion, they are ineffective against TLC due to their low vapor pressure [11,12].

Studying VPC, especially under a thin liquid film, requires a complex experimental setup. Several setups have been proposed over the years, but they often have limitations. For example, one commonly used method for TLC monitoring in laboratories is the weight loss coupon technique. In this method, a coupon is flush-mounted on a lid, with its temperature controlled externally. Corrosion occurs on the coupon's downward-facing surface, and the rate is measured by weighing the coupon after removing the corrosion product [13]. This technique measures both uniform and localized corrosion over time, but it only provides cumulative data at the end of the exposure period. In 2010, Gunaltun et al. [14] evaluated the effectiveness of VCIs using several innovative experimental setups, including the Electrical Resistance (ER) probe. However, the ER probe required the sensing element to remain fully wet to collect meaningful data. In 2013, Sunder Ramachandran et al. [15] explored the quartz crystal microbalance (QCM) technique, which measures surface mass changes with high accuracy. While this method can detect minute changes from nanograms to micrograms, technical challenges remain in adapting it to simulate real-world conditions.

It was initially believed that the low conductivity of condensed water would hinder the use of Linear Polarization Resistance (LPR) probes. In 2012, however, Oehler et al. [16] proposed a "cold finger probe" to monitor VCI efficiency using the LPR technique. Their setup involved carbon steel pins exposed to the corrosive vapor phase. Condensed water was collected and used for LPR measurements. However, this setup did not accurately represent the condensation rate and temperature.

This manuscript, therefore, aims to develop a novel experimental setup that simulates pure top-of-the-line conditions, with customized control over condensation rates, temperature, and droplet retention time. This setup will enable in-situ measurements of TLC. Subsequently, the performance of VCIs will be evaluated using this newly designed setup.

2. Experimental procedure

Construction of TLC probe

The TLC probe was designed based on methods outlined in a prior study ®. It consisted of two carbon steel rods with identical chemical compositions (0.30% carbon, 0.75% manganese, 0.25% silicon, 0.04% phosphorous, 0.04% sulfur, and the balance being iron), as depicted in Figure 1. The larger rod, measuring 20 mm (0.79 in) in diameter and 30 mm (1.18 in) in length, was drilled to create a central hole with a 3 mm (0.12 in) diameter.

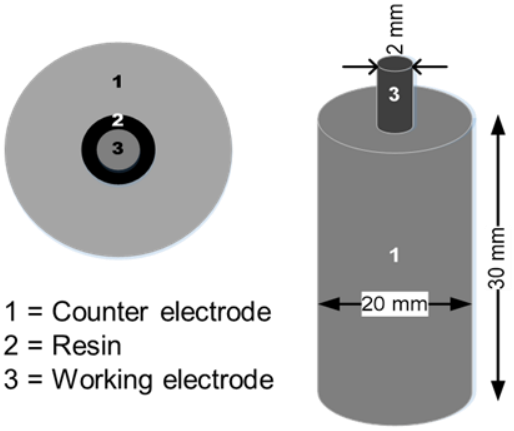

Figure 1. Schematic of top-of-the-line corrosion (TLC) probe

The smaller rod was machined to dimensions of 2 mm (0.08 in) in diameter and 40 mm (1.57 in) in length. Both rods underwent sandblasting and were thoroughly cleaned using water and acetone before being air-dried.

Subsequently, a layer of cationic epoxy (Powercron™ 6000CX) was applied to the rods, which were then cured in an oven at 150 °C for 20 minutes. After curing, the smaller rod was inserted into the hole of the larger rod, and the annular gap was filled with epoxy. In this setup, the smaller rod functioned as the working electrode, while the larger rod served as the counter/reference electrode. Both components were electrically insulated with a layer of cationic epoxy and epoxy resin. Prior to experimentation, the probe's flat surface was polished with silicon carbide paper up to 1200 grit. It was then washed with water, rinsed with ethanol, and dried using a laboratory drying oven. Finally, the dried probe was mounted into the TLC setup.

Construction of TLC cell

Figure 2 illustrates the configuration of our TLC setup. The prepared TLC probe was inserted into the polyethylene terephthalate (PET) lid, with its polished surface facing downward toward the corrosive environment, while the upper portion extended above the lid. This assembly included temperature sensors for monitoring both the gas and surface temperatures, a thermocouple to regulate the bulk liquid temperature, a CO_2 inlet, and a cup to collect the condensed liquid. A copper coil was wrapped around the upper section of the probe, through which cooling liquid circulated to maintain the desired surface temperature. A temperature sensor was positioned in a small hole just above the polished section of the TLC probe to record surface temperature, while another sensor, suspended in the vapor phase, measured the gas temperature. The entire system was mounted on a 3.5 L stainless steel container to create a sealed environment. High-purity CO_2 gas (99.99%) was continuously bubbled through the setup for 24 hours to deoxygenate the system. To avoid oxygen contamination, 1000 mL of distilled water—pre-sparged overnight with CO_2 and pre-heated to the target temperature—was transferred to the TLC cell using a peristaltic pump. The desired gas and surface temperatures were regulated by controlling the bulk liquid and cooling water temperatures, respectively. In this experiment, the surface temperature was held constant at 30°C, while gas temperatures were varied at 40°C, 50°C, and 60°C. Condensed liquid, which collected in a container beneath the sample, was quickly transferred to a reservoir at room temperature to prevent re-evaporation. The liquid from the reservoir was then analyzed to measure its mass, inhibitor concentration, and ferrous ion (Fe^{2+}) levels. The water condensation rate was calculated by dividing the volume of collected liquid by the probe's exposed surface area and the time elapsed. In-situ TLC rates were determined using the Linear Polarization Resistance (LPR) method, as well as by measuring Fe^{2+} concentration in the condensed liquid over a 24-hour period, with and without inhibitors. Spectrophotometric technique was employed to measure Fe^{2+} concentration in the condensed liquid. The test matrix for LPR measurement is depicted in Table 1. Each experiment was conducted at least twice, and the average values, along with standard deviations, were reported.

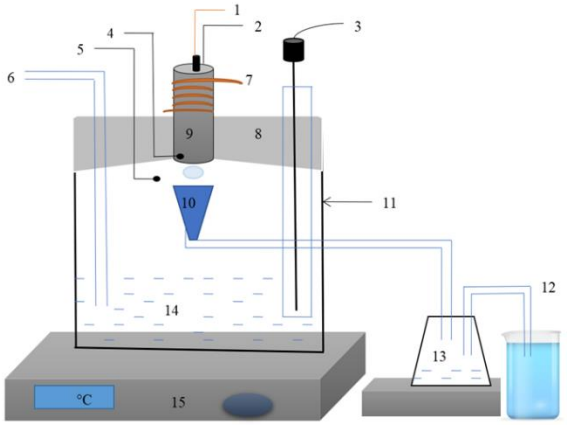

Figure 2. Schematic of top-of-the-line corrosion (TLC) setup; 1. Working electrode connection, 2. Counter/reference connection, 3. Thermocouple, 4. Surface temperature probe, 5. Gas temperature probe, 6."CO_2" inlet, 7. Cooling coil for maintaining surface temper, 8. Polyethylene terephthalate lid, 9. TLC probe, 10. Condensate collector, 11. 3.5-L stainless steel vessel, 12.CO_2 outlet, 13. Condensate reservoir, 14. Distilled water, 15. Heater

Table 1. Experimental conditions for LPR measurement

Parameters	Conditions
Bulk liquid	CO_2 saturated distilled water
Sample surface temperature	30°C
Vapour temperature	50°C
Corrosion inhibitor	Benzothiazole
Inhibitor concentration	200 ppm, 500 ppm and1000 ppm
Test duration	1 day
Measurement	LPR

Electrochemical Measurements

All electrochemical measurements were conducted using a two-electrode configuration. The working electrode was connected to the central carbon steel rod of the TLC probe, which served as the working electrode, while the counter and reference ports were short-circuited and linked to the counter electrode. These measurements were performed using a Gamry Instrument Potentiostat/Galvanostat/ZRA (Reference 620). Data plotting, graphing, and fitting were done through the Echem Analyst Software. Linear Polarization Resistance (LPR) tests were carried out within a range of ±5 mV

relative to the open circuit potential (OCP), with a scan rate of 10 mV/min.

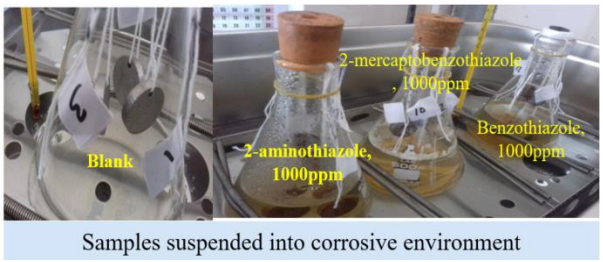

Figure 3. Screening of VCIs by simple vapour inhibiting ability (VIA) test

Table 2. Experimental conditions for vapour inhibiting ability (VIA) test

Parameters	Conditions
Bulk liquid	Distilled water
Liquid temperature	50°C
Vapour temperature	40°C
Corrosion inhibitors	2-aminothiazole, 2-mercaptobenzothiazole and Benzothiazole
Inhibitor concentration	1000 ppm
Test duration	3 days
Measurement	Weight loss (WL)

Vapour inhibiting ability (VIA) test

The Vapor Inhibiting Ability (VIA) test was used to identify potential volatile corrosion inhibitors (VCIs) among three azole derivatives: 2-aminothiazole, 2-mercaptobenzothiazole, and benzothiazole. The VIA test setup is shown in Figure 3 and the test matrix is mentioned in Table 2. Four 250 mL conical flasks were used for the experiment. Three flasks were filled with 100 mL of different inhibitor solutions, and one was filled with 100 mL of water as a control for the blank experiment. Carbon steel samples were prepared by polishing them with silicon carbide paper down to 1200 grit. Each sample was weighed individually before being suspended in the corrosive environment. Two samples were suspended in the vapor phase, and two were suspended in the immersion phase, each placed separately in its respective conical flask. At the end of the test period, all samples were cleaned using hydrochloric acid (HCl) containing hexamethylene, following ASTM standards, and weighed again. The inhibition efficiency (∈) was then calculated using the following equation:

$$\in = \frac{CR_o - CR_i}{CR_o} \times 100$$

where ∈ is the efficiency of inhibitor, $CR_o$is the corrosion rate without inhibitor and $CR_i$is the corrosion rate with inhibitor.

3. Results and discussion

Controlling of surface temperature and gas temperature

To effectively study TLC, it is crucial to precisely control both the sample surface temperature and the gas temperature, as water condensation rates—one of the key factors influencing TLC—are directly dependent on these two variables. Additionally, the kinetics of corrosion are significantly affected by the surface temperature. Previous research indicated that at lower surface temperatures, TLC rates were independent of condensation rates, whereas at higher temperatures, TLC rates increased with higher condensation rates [4]. However, very few studies have managed to control these temperatures accurately. In our newly developed TLC setup, the surface temperature was regulated by externally cooling the sample, while the gas temperature was controlled by adjusting the bulk liquid temperature. Both temperatures were measured using thermocouple probes and recorded in a data logger throughout the experimental period. Figure 4 illustrates the stability of the surface and gas temperatures during the experiment. In this study, the surface temperature was consistently maintained at 30°C, while the gas temperature was varied at 40°C, 50°C, and 60°C.

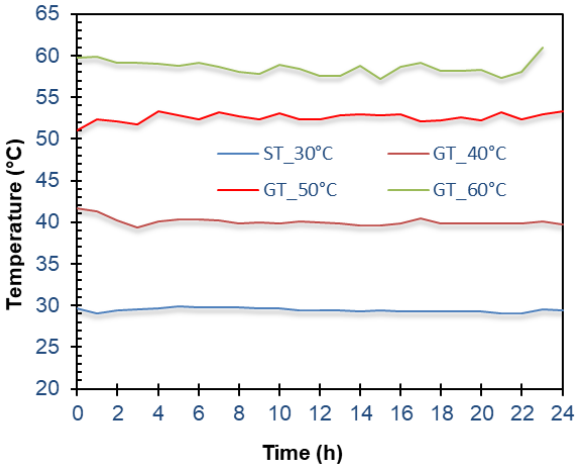

Figure 4. Constantly recorded sample surface temperature and gas temperature

Droplet Retention Time (DRT) and Water Condensation Rate (WCR)

The droplet retention time (DRT) refers to the duration for which a water droplet remains in contact with a steel surface before detaching due to the force of gravity. Although DRT is inversely proportional to the water condensation rate (WCR), WCR only provides an estimate of droplet longevity, not the precise duration of contact. Therefore, understanding DRT is crucial, as it may provide insights into the mechanism of TLC, particularly because the water chemistry within a droplet evolves over time. In previous work, Islam et al. measured DRT by placing a temperature probe beneath the sample surface, monitoring the changes in droplet temperature from initiation to termination [4]. However, implementing such a temperature probe in actual pipeline scenarios is impractical. To address this, a different technique was employed in this study—measuring the open circuit potential (OCP) using an electrochemical probe.

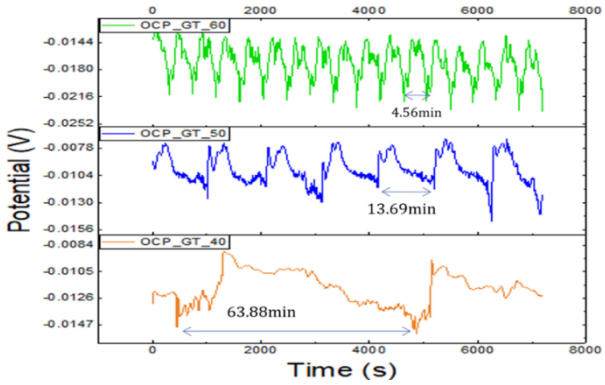

Figure 5. The OCP of the sample at variable gas temperature of 40, 50 and 60 °C

Figure 5 displays the fluctuations in OCP of carbon steel when suspended within a condensed water droplet. Initially, the OCP of the sample gradually decreased as the droplet grew. Once the droplet detached from the surface, the OCP reading returned to its initial value, marking the formation of a new droplet. In other words, each droplet cycle exhibited a maximum OCP, signifying droplet initiation, and a minimum OCP, indicating when the droplet fell. The interval between two minimum OCP readings represented the DRT. Several intervals were recorded for each condition, and the average DRT values were reported. The water condensation rate (WCR) was calculated by dividing the mass of condensed water collected by the surface area and time. Table 1 summarizes the average DRT and WCR under different experimental conditions. As expected, the shortest DRT of 4.56 minutes was observed at the highest WCR of 1.44 g m^{-2} s^{-1}, with a gas temperature (GT) of 60°C and a surface temperature (ST) of 30°C. The lowest WCR of 0.28 g m^{-2} s^{-1} was recorded at a GT of 40°C and ST of 30°C.

Table 3. Droplet Retention Time (DRT) and Water Condensation Rate (WCR) at 40, 50 and 60°C

Condition	Droplet retention time (min)	Water condensation rate ($gm^{-2}s^{-1}$)
GT_40°C	63.88	0.28
GT_50°C	13.69	0.51
GT_60°C	4.56	1.44

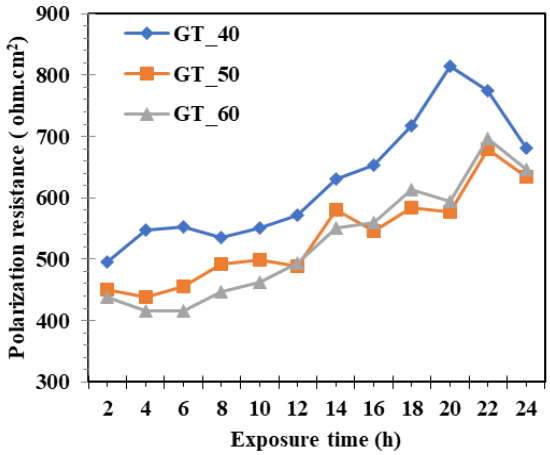

Figure 6. Polarization resistance of TLC probe under CO_2 condition

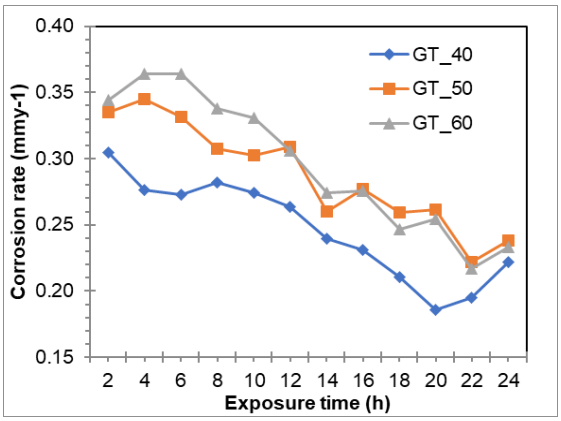

Figure 7. Top of the line corrosion (TLC) rate

Measurement of TLC rate using newly designed setup

The TLC rate was determined using both electrochemical linear polarization techniques and by measuring the iron concentration in the condensed liquid. During the experiments, the surface temperature (ST) was held constant at 30°C, while the gas

temperature (GT) was varied at 40°C, 50°C, and 60°C. Figure 6 presents the polarization rates of the TLC probe under CO_2 conditions over a 24-hour period. These polarization rates were then converted into corrosion rates using the Stern-Geary equation, as shown in Figure 7. As expected, the TLC rates increased with rising gas temperatures, which can be attributed to the corresponding increase in condensation rates.

Vapour inhibiting ability (VIA) test results

The VIA test provides semi-quantitative information regarding the effectiveness of vapour phase corrosion inhibitors in preventing corrosion. Figure 8 illustrates the inhibition efficiencies of 2-aminothiazole, 2-mercaptobenzothiazole, and benzothiazole under both vapour phase and immersion conditions. The results indicate that all three compounds—2-aminothiazole, 2-mercaptobenzothiazole, and benzothiazole—are equally effective in inhibiting corrosion under immersion conditions, achieving an inhibition efficiency of approximately 90%. However, under vapour phase conditions, benzothiazole exhibits superior performance with an inhibition efficiency of 53%, outperforming the other two compounds. Consequently, benzothiazole was selected for further investigation under TLC conditions to evaluate its efficacy.

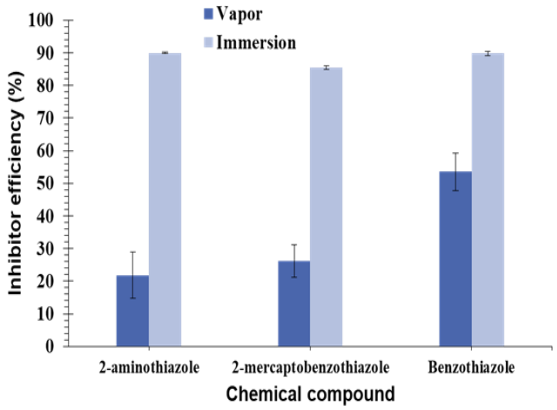

Figure 8. Inhibition efficiency of 2-aminothiazole, 2-mercaptobenzothiazole and Benzothiazole in both condition vapour and immersion

Table 4. Average Inhibition efficiency of 2-aminothiazole, 2-mercaptobenzothiazole and Benzothiazole

Azole derivative	(%) Inhibitor efficiency	
	Vapour phase	Immersion phase
2-aminothiazole	21.82	89.97
2-mercaptobenzothiazole	26.20	85.40
Benzothiazole	53.50	89.77

Inhibition efficiency of Benzothiazole under TLC condition

Benzothiazole was introduced into the newly designed TLC setup, where the TLC rate was assessed using the linear polarization technique and by measuring the iron concentration in the condensed liquid. Figure 9 illustrates the polarization resistance of the carbon steel sample obtained from the TLC system over one day, maintaining a surface temperature of 30 °C and a gas temperature of 50 °C in a CO_2 corrosion environment. Benzothiazole concentrations of 200 ppm, 500 ppm, and 1000 ppm were tested. The results clearly show that polarization resistance increases with higher inhibitor concentrations. A greater polarization resistance indicates a reduced likelihood of corrosion on the surface. The maximum polarization resistance was observed when 1000 ppm of benzothiazole was injected into the CO_2 corrosion system compared to the other concentrations. The polarization resistance values were converted into inhibition efficiency, as depicted in Figure 10. It is evident that the inhibition efficiency of benzothiazole is concentration-dependent, with the highest inhibition efficiency occurring at 1000 ppm. This indicates that the inhibitor concentration significantly influences the reduction of the TLC rate.

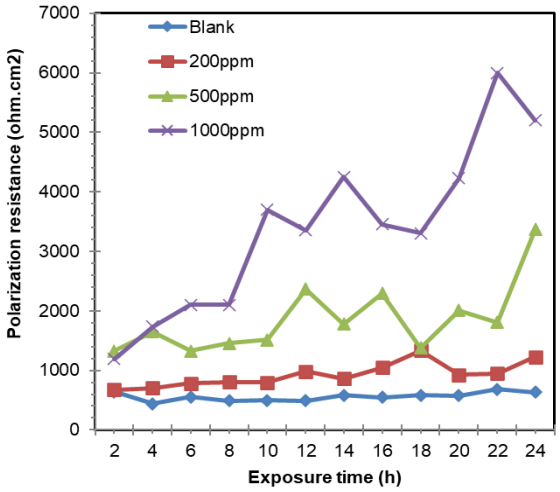

Figure 9. Polarization resistance of carbon steel sample

The average inhibition efficiency, as illustrated in Table 5, increased from 38% to a maximum of 80% as the inhibitor concentration rose from 200 ppm to 1000 ppm. Additionally, the inhibition efficiency of benzothiazole was calculated based on the Fe^{2+} concentration measured in the collected condensed liquid. In the collected condensed liquid, iron (II) reacts with 1,10-phenanthroline (ortho-phenanthroline) to form an

orange-red complex {Ferrous ortho-phenanthroline-$[(C_{12}H_8N_2)_3Fe]^{2+}$}, which exhibits maximum absorbance at a wavelength (λmax) of 510 nm. The iron concentration was then converted into the total iron amount in the collected condensed liquid, which is considered the weight loss of the carbon steel sample. Consequently, the inhibition efficiency was calculated from the weight loss, as illustrated in Figure 11. The highest inhibition efficiency from the experiments was observed when using 1000 ppm of the inhibitor.

Table 5. Average Inhibition efficiency of Benzothiazole

Chemical compound		(%) Inhibitor efficiency
	Concentration	
Benzothiazole	200 ppm	38
	500 ppm	68
	1000 ppm	80

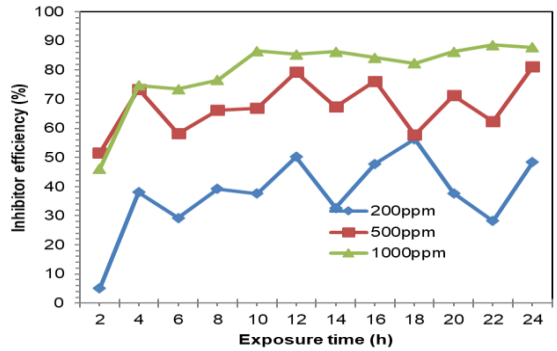

Figure 10. Inhibition efficiency of Benzothiazole

Measurement of inhibitor concentration in the condensed liquid

Measuring the concentration of the inhibitor in the condensed liquid is both crucial and challenging. We did not identify any previous studies that have measured inhibitor concentration in condensed liquids; thus, we are proposing this method for the first time. The UV spectra of the benzothiazole standard solution and the benzothiazole collected from the condensed liquid sample are presented in Figure 12. The maximum absorption was detected at a wavelength of 228 nm, and no additional absorption peaks were observed for the presence of Fe^{2+} ions in the condensed liquid. This suggests that Fe^{2+} does not interfere with the measurement of benzothiazole. A standard curve correlating absorption with concentration at the 228 nm wavelength was created, as shown in Figure 13. The concentration of benzothiazole in the condensed liquid was subsequently determined using this standard curve.

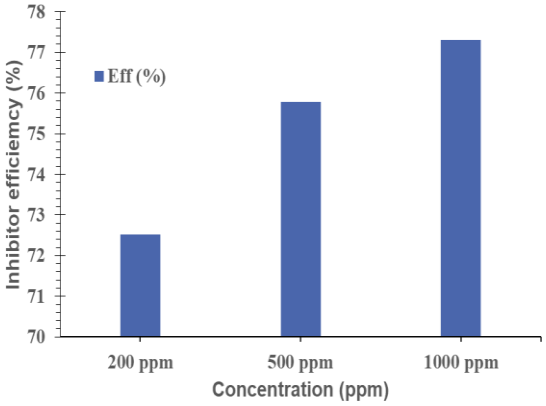

Figure 11. Inhibition efficiency of Benzothiazole

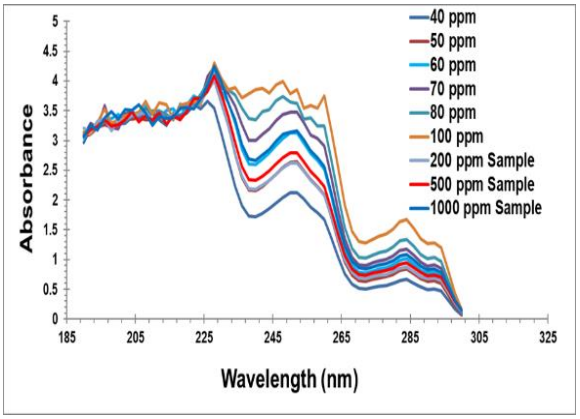

Figure 12. UV-spectrum of Benzothiazole

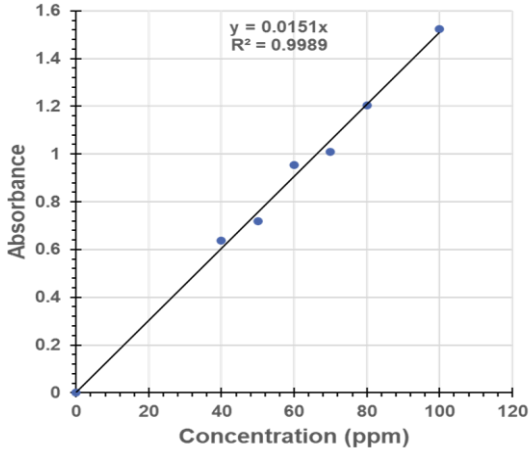

Figure 13. Standard curve for spectrophotometric determination of benzothiazole

Table 6 summarizes the concentrations of benzothiazole found in the condensed liquid. Notably, as the benzothiazole concentration in the bulk liquid increased from 200 ppm to 1000 ppm, the concentration in the condensed liquid rose from 213 ppm to 263 ppm. This higher concentration of benzothiazole in the condensed

liquid suppresses the TLC rate by forming a barrier film on the sample surface.

Table 6. Benzothiazole concentration (ppm) in the condensed liquid

Chemical compound	Inhibitor concentration (ppm)	
	In sample	In condensed liquid
Benzothiazole	200	213
	500	250
	1000	263

4. Conclusions

- The newly designed TLC cell setup effectively measures top-of-the-line corrosion (TLC) using the linear polarization technique and quantifies Fe^{2+} concentration in the collected condensed liquid. This setup also measures condensation rates, droplet retention times, and allows precise control of both sample surface temperature and gas temperature.
- Simple vapour inhibiting ability (VIA) tests indicate that 2-aminothiazole, 2-mercaptobenzothiazole, and benzothiazole can effectively prevent bottom-of-the-line corrosion, achieving an inhibition efficiency exceeding 85%. However, for top-of-the-line corrosion, benzothiazole demonstrates superior efficiency (53%) compared to the other inhibitors, making it a promising candidate for mitigating vapour phase corrosion.
- Under top-of-the-line conditions, the inhibition efficiency of benzothiazole is concentration-dependent, as determined by our newly designed TLC setup. Maximum inhibition efficiency under TLC condition is found to reach about 80% at 1000 ppm.
- For the first time, a straightforward method has been introduced for determining inhibitor concentration in the collected condensed liquid. It reveals that a significant amount of inhibitor is co-condensed with water.

Funding

This work was supported by the Director of Research and Extension of Rajshahi University of Engineering and Technology [grant numbers DRE/7/RUET/528 (39)/pro/2021–2022/31, 2021].

References

[1] M. J. Mazumder, "Global Impact of Corrosion: Occurrence, Cost and Mitigation," Global Journal of Engineering Sciences, vol. 5, no. 4, pp. 1-5, June 2020.

[2] S. Gangopadhyay and P. A. Mahanwar, "Recent developments in the volatile corrosion inhibitor (VCI) coatings for metal: a review," Journal of Coatings Technology and Research, vol. 15, no. 4, pp. 789-807, May 2018.

[3] M. M. Islam, T. Pojtanabuntoeng, and R. Gubner, "Corrosion of carbon steel under condensing water and monoethylene glycol," Corrosion Science, vol. 143, pp. 10-22, July 2018.

[4] M. M. Islam, T. Pojtanabuntoeng, and R. Gubner, "Condensation corrosion of carbon steel at low to moderate surface temperature and iron carbonate precipitation kinetics," Corrosion Science, vol. 111, pp. 139-150, May 2016.

[5] I. Jevremović, M. Singer, M. Achour, D. Blumer, T. Baugh, V. Misković-Stanković, and S. Nešić, "A novel method to mitigate the top-of-the-line corrosion in wet gas pipelines by corrosion inhibitor within a foam matrix," Corrosion Science, vol. 69, no. 2, pp. 186-192, February 2013.

[6] F. A. Ansari, C. Verma, Y. S. Siddiqui, E. E. Ebenso, and M. A. Quraishi, "Volatile corrosion inhibitors for ferrous and non-ferrous metals and alloys: A review," International Journal of Corrosion and Scale Inhibition, vol. 7, no. 2, pp. 126-150, March 2018.

[7] D. M. Bastidas, E. Cano, and E. M. Mora, "Volatile corrosion inhibitors: A review," Anti-Corrosion Methods and Materials, vol. 52, no. 2, pp. 71-77, April 2005.

[8] Z. Chen, L. Huang, G. Zhang, Y. Qiu, and X. Guo, "Benzotriazole as a volatile corrosion inhibitor during the early stage of copper corrosion under adsorbed thin electrolyte layers," Corrosion Science, vol. 65, pp. 214-222, December 2012.

[9] M. Edraki and D. Zaarei, "Azole derivatives embedded in montmorillonite clay nanocarriers as corrosion inhibitors of mild steel," International Journal of Minerals, Metallurgy, and Materials, vol. 26, no. 1, pp. 86-97, January 2019.

[10]E. B. Caldona, M. Zhang, G. Liang, T. K. Hollis, C, E. Webster, D. W. Smith Jr, and D. O. Wipf, "Corrosion inhibition of mild steel in acidic medium by simple azole-based aromatic compounds," Journal of Electroanalytical Chemistry, vol. 880, pp. 114858, November 2021.

[11]Y. P. Asmara, V. Suraj, J. P. Siregar, T. Kurniawan, D. Bachtiar, and N. M. Z. N. Mohamed, "Development of green vapour corrosion inhibitor," 4th International Conference on Mechanical Engineering Research (ICMER), pp. 012089, Pahang, Malaysia, 2017.

[12]V. Vorobyova, O. Chygyrynets, M. Skiba, T. Zhuk, I. Kurmakova, and O. Bondar, "A comprehensive study of grape pomace extract and its active components as effective vapour phase corrosion inhibitor of mild steel," International Journal of Corrosion and Scale Inhibition, vol. 7, no. 2, pp. 185-202, May 2018.

[13]M. Singer, A. Camacho, B. Brown, and S. Nešić, "Sour top-of-The-line corrosion in the presence of acetic acid," Corrosion, vol. 67, no. 8, pp. 085003-1, August 2011.

[14]Y. S. Gunaltun, E. P. Tong, M. Singer, C. Duret, and S. Espitalier, "Laboratory testing of volatile corrosion inhibitors," CORROSION 2010 Conference & Expo, NACE - International, San Antonio, Texas, 2010.

[15]S. Ramachandran, V. Jovancicevic, P. Rodgers, I. Ahmed, H. Vance, and M. Al-Waranbi, "A New Top-of-the-Line Corrosion Inhibitor to Mitigate Carbon Dioxide Corrosion in Wet Gas Systems," CORROSION 2013 Conference & Expo, NACE - International, Orlando, Florida, 2013.

[16]M. C. Oehler, S. I. Bailey, R. Gubner, and M. Gough, "Testing of Generic Volatile Inhibitor Compounds in Different Top-of-the-Line Corrosion Laboratory Test Methods," CORROSION 2012 Conference & Expo, NACE - International, Salt Lake City, Utah, 2012.